HHS Public Access

Author manuscript

Nanomedicine. Author manuscript; available in PMC 2024 July 30.

Published in final edited form as:

Nanomedicine. 2019 October ; 21: 102049. doi:10.1016/j.nano.2019.102049.

Evaluation of an adjuvanted hydrogel-based pDNA nanoparticulate vaccine for rabies prevention and immunocontraception

Amit Bansal[a], **Wael Gamal**[a], **Xianfu Wu**[b], **Yong Yang**[b], **Victoria Olson**[b], **Martin J. D'Souza**[a]

[a]Center for Drug Delivery Research, Vaccine Nanotechnology Laboratory, Mercer University, College of Pharmacy, Atlanta, GA, 30341 USA

[b]Poxvirus and Rabies Branch, DHCPP, NCEZID, Centers for Disease Control and Prevention, Atlanta, GA, 30329 USA

Abstract

Immunocontraceptive vaccination is becoming an acceptable strategy in managing animal populations. Mass vaccination of dogs is the most cost-effective and efficient method to control rabies, and combination of rabies vaccination and animal population control will be an added advantage. In this study, we developed an adjuvanted hydrogel-based pDNA nanoparticulate vaccine for rabies protection and immunocontraception. *In vivo*, we observed an immune response skewed towards a Th2 type, in contrast to the Th1 type in our previous pDNA study. The observation was verified by the IgG2a/IgG1 ratio (<1), and cytokine expression profile of IL-4 and IFN-ϒ. The humoral immune response is key for rabies protection and a GnRH antibody-based immunocontraception. In mice, anti-GnRH antibody titers were detected 4 weeks after immunization and lasted for 12 weeks when the animal experiment was terminated. The adjuvanted pDNA nanoparticulate vaccine shows promise for future studies evaluating protection from rabies challenge and prevention of animal breeding.

Graphical Abstract

Correspondence: Martin J. D'Souza, 3001 Mercer University Drive, DV-108, Atlanta, GA 30341, Fax 678 547 6364, dsouza_mj@mercer.edu.

Disclosure

The authors report no conflicts of interest in this work. The authors alone are responsible for the content and writing of this article.

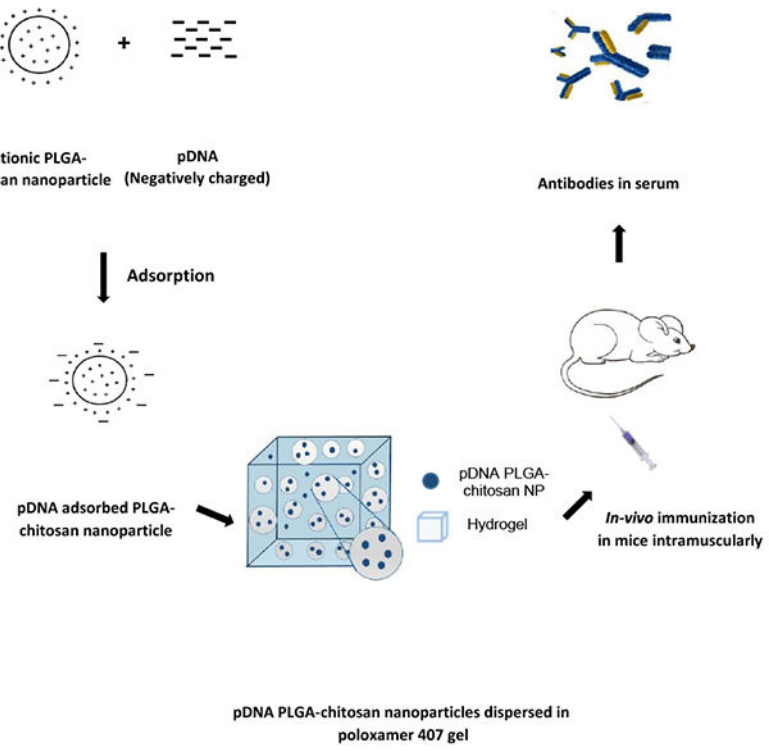

Schematic procedure used for the adsorption of pDNA on cationic nanoparticles, further dispersion in hydrogel and immunization in mice

Keywords

Immunocontraceptive vaccine; Gonadotrophin-releasing hormone (GnRH); Rabies; Poloxamer Gels

INTRODUCTION

Rabies prevention is an excellent example of “one health” involving animals, humans and the environment. Rabid dog bites account for about 95% of human rabies cases in the 55,000 human deaths reported per year worldwide [1] [2]. Elimination of dog-mediated human rabies deaths by 2030 is a goal set by WHO and OIE [5], and there is a need for coordinated efforts and development of novel stratgies to contain the spread of rabies. More than 3.3 billion people in endemic countries live in an environment with potential exposure to rabies [3]. Besides mass dog vaccinations, novel vaccine formulations and delivery are being explored [4]. An efficient canine rabies control program relies on dog vaccination and population management [6,7], particularly for free-roaming dogs. Dog culling is not only often unacceptable to the community, but also proves ineffective in rabies control [7]. The Alliance for Contraception in Cats and Dogs (ACC&D) strongly recommends the use of nonsurgical method for control of animal population [6].

The pDNA is an immunocontraceptive vaccine, and has the advantages of being inexpensively produced, stable at room temperature, relatively safe and capable of inducing both humoral and cellular immune responses [8]. But unmodified DNA vaccines come with an inherited limitation of weak immunogenicity. Similarly, immunocontraception is less expensive and less labor-intensive than the surgical method for sterilization, but the effect is not as reliable, with most studies still in the research stage. One method of achieving immunocontraception is by targeting gonadotrophin-releasing hormone (GnRH), a neuronal hormone secreted in the hypothalamus and transported to the anterior pituitary via the hypothalamic-pituitary portal system [9] [10]. After binding to the receptor, GnRH stimulates the production and release of pituitary hormone follicle stimulating hormone (FSH) and luteinizing hormone (LH), which play a critical role in the development of sexual organs and reproduction [11] [12]. Antibodies against GnRH prevent its binding to the receptor and thus inhibit secretion of FSH and LH to achieve sterility. Both male and female animals have been shown to respond well to the GnRH vaccine, with above 80% infertility in animal breeding, and no serious social behavior changes have been observed in the immunized animals [13, 14].

Development of a DNA vaccine to generate antibodies to prevent GnRH signalling is challenging due to its weak immumogeniciy [20]. To overcome the limitation, various strategies have been employed, including coupling of GnRH to ligands such as heat shock protein 65 [21], keyhole limpet hemocyanin [22] and stronger T helper cell epitopes [23]. Similarly, we attempted to elongate the length of time the antigen was present within the animal by developing a hydrogel-based pDNA nanoparticulate vaccine. The vaccine formulation in our study maintained a fluid state at 4^{o}C, thus providing ease of administration, but turned into a gel after injection in animals, thus providing a method for sustainable release of the antigen. To further augment the vaccine immunogenicity, we included the FDA-approved adjuvants Alum and MF59 in our vaccine formulations [24, 25].

MATERIALS AND METHODS

Cell culture materials RPMI 1640 medium, Dulbecco’s Modified Eagle medium, fetal bovine serum (FBS), penicillin/streptomycin, sodium pyruvate and nonessential amino acids were obtained from Cellgro Mediatech (Herndon, VA, USA). Mouse dendritic DC 2.4 cells were given as a kind gift from Dr. Kenneth L. Rock (Dana-Farber Cancer Institute, Inc., Boston, MA, USA). Six to eight week-old Swiss Webster female mice were purchased from Charles River Laboratories (Wilmington, MA, USA). GnRH peptide conjugated to BSA was bought from New England Peptide, Inc. (Gardner, MA, USA). Antibodies used to stain cells for MHC I, MHC II, IFN-ϒ, IL-4, CD45R, CD62L, CD4 and CD8 for flow cytometry analysis were purchased from eBioscience laboratories (San Diego, CA, USA). HRP-tagged secondary goat anti-mouse IgG was procured from Invitrogen (Rockford, IL, USA). Bovine serum albumin (BSA), polyvinyl alcohol, dichloromethane, and PLGA (Mw 7,000-17,000) were purchased from Sigma (St Louis, MO, USA). Chitosan glutamate (Sea Cure (+) 210) was purchased from Protan, Inc. (Portsmouth, NH, USA).

Immunization of mice

To determine the antigenicity of pDNA nanoparticulate vaccine, 18 Swiss Webster female mice were immunized and housed under specific pathogen-free conditions in accordance with the approved Mercer University IACUC protocol. Mice were divided into three groups; the first group (n=6) received pDNA in hydrogel, the second group (n=6) received pDNA nanoparticulate vaccine in hydrogel and the third group (n=6) received pDNA nanoparticulate vaccine with adjuvants (Alum and MF59) in hydrogel. Mice were immunized intramuscularly with one prime dose of pDNA at 100 μg on day 0. Sera were collected weekly up to twelve weeks after the prime immunization to measure specific antibody levels against GnRH.

Fabrication of PLGA-chitosan nanoparticles

Nanoparticles were prepared by the emulsification method. Briefly, 50 mg of PLGA (Mw 7,000-17,000) was added to 5 mL of dichloromethane (DCM), which comprised the organic phase. The aqueous phase was prepared by mixing 1 mg of polyvinyl alcohol (PVA) in deionized water (Millipore, Billerica, MA, USA) and was then added to the organic phase under homogenization at a speed of 32,000 rpm to form a w/o (water/oil) emulsion. The formed w/o emulsion was later added to the second aqueous phase containing 10 mg of polyvinyl alcohol (PVA) and 20 mg of chitosan glutamate under homogenization at a speed of 32,000 rpm to form a w/o/w multiple emulsion that was kept stirring overnight. The nanoparticle suspension was washed twice with deionized water to remove excess PVA. Finally, the suspension was freeze-dried using trehalose (Sigma, St Louis, MO, USA) as a cryoprotectant and the nanoparticles were characterized for their size and zeta potential [27] [8].

Measurement of particle size & zeta potential

The particle size of the optimized nanoparticulate formulation was determined by a Malvern Zetasizer Nano ZS (Worcestershire, UK) that works on the principle of dynamic light scattering. One mg of nanoparticles was suspended in 1 mL of deionized water, vortexed and then analyzed for size. The measurement was done in triplicate for blank nanoparticles and pDNA vaccine nanoparticles. The zeta potential of optimized nanoparticulate formulation was similarly determined. One mg of nanoparticles was suspended in 1 mL of deionized water and transferred to a cuvette, and measured using a Malvern Zetasizer [8].

Dye exclusion assay

Measurement of the condensation of pDNA by chitosan glutamate was determined by quenching of ethidium bromide (EtBr) fluorescence [28]. Briefly, 1 μg of pDNA was added to wells of a 96-well plate and later a solution of chitosan glutamate (50 μL) in HBG buffer (20 mM Hepes, 5.2% glucose, pH 7.0) was added in increasing concentrations (0.1-0.5 μg/μL) to the pDNA-treated wells. Samples were incubated for 30 minutes and 50 μL of EtBr (2.5 μM) was added to each well. The same procedure was followed for the different ratios of nanoplex (P/N, 1/15, 1/30, 1/45, 1/50) in which each P/N sample in HBG buffer was incubated with 50 μL of EtBr (2.5 μM) for 30 min. The wells containing only pDNA and HBG buffer were treated as positive and negative controls, respectively. All

measurements were performed in triplicate and fluorescence intensity was measured in a microplate reader (BioTek instruments Inc., Winooski, VT) using an excitation wavelength of 510 nm and an emission wavelength of 591 nm [29] [30].

Griess nitrite assay

Determination of nitric oxide production was achieved by measuring its oxidation product nitrite via Griess reaction [8]. Adherent DC 2.4 cells were suspended in Dulbecco's complete media and dispensed to wells of 96-well flat-bottomed plate at a density of 2.0×10^4/well. Samples from different vaccine groups used in the study (i.e., pDNA, blank NP, pDNA nanoparticulate vaccine) with or without adjuvants were incubated with DC cells for 16 hrs and 24 hrs at 37 °C under 5% CO_2. Lipopolysaccharide (LPS) was used as positive control. Supernatants were collected and added to wells of another 96-well plate (50 μL) in triplicate for detection of nitrite (NO_2) accumulated in supernatants of induced DC 2.4 cells. To perform the measurement, 50 μL of 1% sulfanilamide in 5% phosphoric acid was added and incubated for 5-10 minutes in the dark, followed by addition of 50 μL 0.1% N-1-napthylethylenediamine dihydrochloride for further incubation for 5-10 min in the dark. The absorbance was read at wavelength of 550 nm by a microplate reader [31] [32]. Nitrite content was quantitated using the standard curve of sodium nitrite: 1 mM stock in distilled water diluted to the high end at 100 μM, followed by serial dilutions to the low end at 1.56 μM.

Quantification of antigen-presenting molecules (MHC I and MHC II) expression

DC 2.4 cells were plated at 5×10^4 cells per well in a 48-well plate and incubated at 37°C for 24 hrs. After incubation, the adherent cells in each well were pulsed with 50 μg vaccine nanoparticles along with adjuvant particles and incubated at 37°C for another 24 hrs. To measure MHC I and MHC II, the remaining extracellular nanoparticles were removed, and the cells were harvested by using a cell scraper. After staining at 4°C for 1 hr with Fluorescein isothiocyanate (FITC) labeled MHC I and MHC II markers, the DC2.4 cells were washed twice with Hanks balanced salt solution (HBSS), and stained markers were measured under the BD Accuri C6 flow cytometer (BD Bioscience, San Jose, CA).

Detection of Anti-GnRH antibodies by ELISA

Enzyme-linked immunosorbent assay (ELISA) was carried out for the detection of specific antibodies against GnRH. Blood samples from immunized mice were collected every week and serum was isolated and analyzed for antibody titers. Briefly, the 96-well flat-bottomed poly-L-lysine coated high binding plate was coated with 1 μg (100 μL/well) of GnRH peptide conjugated to BSA (GnRH-BSA) and kept overnight at 4°C. Wells were blocked with 5% (w/v) BSA in phosphate buffered saline (PBS, 0.01M, pH 7.2) at room temperature (RT) for 2 hrs. After extensive washing with PBS containing 0.05% Tween-20 (PBST), 100 μL of serum at 1:100 in PBS containing 5% (w/v) BSA were added to each well. After 2 hrs of incubation at RT and subsequent wash using PBST, HRP-tagged secondary goat anti-mouse IgG at 1:2,000 in PBS containing 5% (w/v) BSA was added to each well for incubation at RT for 1 hr. The color was developed by adding 100 μL/well of 3,3′,5,5′′-tetramethyl-benzidine (TMB) 2.08 mM in the dark for 30 min. The reaction was stopped by adding 50 μL of 2M H_2SO_4 to each well, and colorization was measured at

wavelength 450 nm using the microplate reader (BioTek instruments Inc., Winooski, VT, USA) [33] [34]. The assays were performed in triplicate and the results expressed as mean ± SEM.

IgG subclass ELISA

The procedure for detection of subclass IgG1, IgG2a was similar to what was used for detection of anti-GnRH IgG as described above. In brief, the HRP-tagged secondary antibodies for IgG1 and IgG2a were diluted at 1:2000 and incubated at RT for 1 hr. After washing and color development under TMB, the reaction was stopped by adding 2M H_2SO_4, and the absorbance values were quantified at 450 nm using the microplate reader (BioTek instruments Inc., Winooski, VT, USA).

Avidity assay by elution ELISA

The avidity (AI) of anti-GnRH antibodies was determined by sodium thiocyanate (NaSCN) elution ELISA assay [35] [16]. The AI was defined as the concentration of NaSCN that resulted in a 50% reduction in absorbance from untreated wells. The value of AI close to 1 correlates to high avidity, while AI close to 0 correlates to low avidity. The procedure for avidity measurement was similar to IgG subclass ELISA, but incorporated an additional step in which 50 μL of NaSCN (a chaotropic compound that interferes with antigen-antibody reaction) at 0.1-0.8M was added to the well after completion of Ag-Ab reactions. The plate was further incubated at RT for 20 min, and the AI was measured by absorbance at 450 nm using the microplate reader (BioTek instruments Inc., Winooski, VT, USA).

Lymphocyte proliferation Assay

Splenocytes were harvested from immunized mice by passing the spleen through a 40-μm strainer. The cells were suspended in RPMI media and seeded in a 96-well plate at 100 μL per well of 1×10^5 cells. The pulsed cells included: a control of PBS, pDNA, pDNA nanoparticulate vaccine, pDNA nanoparticulate vaccine plus adjuvant, and a positive control of concanavalin A at 5 μg/mL. After incubation for 2 days at 37°C in a 5% CO_2 incubator, cell proliferation was determined by using Alamar blue, a cell viability assay reagent. The cell supernatants were removed and replaced with media containing Alamar blue for incubation at 37 °C for 2 hrs. The stimulation index was calculated as a ratio of fluorescence intensity of antigen-stimulated cells to the unstimulated cells [36].

Determination of T cells, B cells, and memory immune response in lymphatic organs

The single cell suspension of the spleens and lymph nodes were made using the 40-μm cell strainer. The viability of cells was checked by trypan blue exclusion method with an automated cell counter (Bio-Rad, Hercules, CA). Viable cells at the concentration of 1×10^6 cells/mL were collected in a 1.7 mL Eppendorf tube for detecting the T cell or B cell markers. For T cell analysis, the anti-mouse CD8 FITC, CD62L APC markers were added to the lymphocytes. For B cell analysis, mouse antibodies against CD45R FITC and CD27 APC were added to the lymphocytes. The reactions were kept in the dark and incubated for 1 hr on ice. After incubation, the cells were spun down and washed twice using PBS (0.01M,

pH 7.2), and were resuspended in 200 μL of the same PBS. The cells were analyzed using the flow cytometer, BD Accuri™ C6 Plus (BD Accuri Cytometers, Ann Arbor, MI) [37].

Intracellular Staining

This method allowed simultaneous analysis of cell surface markers by combining fixation and permeabilization in a single step. Immune cells were harvested from mouse spleen, and single cell suspension was prepared by using a 40-μm cell strainer. The cells were first cultured for 3 hrs in complete DMEM supplemented with 2-mercaptoethanol at 50 μM, followed by incubation for 1 hr in the presence of brefeldin at 1μg/mL. After washing cells, $CD4^+$ T cell-FITC was added for incubation for 1 hr. The cells were harvested by centrifugation at 350xg for 5 min, washed twice in PBS (0.01M, pH 7.2), and resuspended in Foxp3 fixation/permeabilization solution for incubation at 4^oC for 30 min in the dark. The cells were pelleted again by centrifugation, and suspended in permeabilization buffer for reaction at RT with IL-4, IFN-Υ APC cytokine markers for 30 min in the dark. After incubation, the cells were washed twice in permeabilization buffer before final resuspension in PBS for analysis using flow cytometry [38] [39].

Statistical Analysis

All experiments were performed in triplicate, unless otherwise indicated. Data analyses were performed using Graphpad Prism version 5 and expressed as mean values ± SEM. One-way ANOVA with Tukey test was used for multiple comparisons. A p value less than 0.05 was considered significant, <0.01 very significant, and <0.001 extremely significant.

RESULTS

Physical characterization of rabies pDNA nanoparticulate vaccine

PLGA nanoparticles were prepared using the emulsification method. Their size ranged from 350-450 nm and the zeta potential varied from -24.0 mV±6.4 mV. Addition of chitosan glutamate at a concentration of 2 mg/mL imparted a positive charge on the surface of nanoparticles up to 50.0 mV and increased the size to 400-500 nm. There was no noticeable physical difference in size of blank nanoparticles versus pDNA-adsorbed nanoparticles. The pDNA alone is negatively charged and the surface of pDNA nanoparticles was positive, indicating complete adsorption of pDNA by chitosan glutamate. Our previous data (not published) revealed that nanoparticles were irregularly-shaped, facilitating uptake by macrophages [40] [41].

Nanoplex P/N at 1/50 was optimal for pDNA condensation

To evaluate chitosan glutamate binding capacity and its optimal concentration in the nanoplex (P/N) for condensation of pDNA, we measured the quenching effect on ethidium bromide fluorescence in the reactions. Figure 1A revealed ethidium bromide fluorescence intensity was not significantly quenched and reached > 70.0% when chitosan glutamate at 0.1 μg/μL and 0.2 μg/μL were added, suggesting the existence of free pDNA in the reaction. After chitosan glutamate increased to 0.3-0.5 μg/μL, the ethidium bromide fluorescence intensity was reduced to < 20.0%. In Figure 1B, fluorescence intensity was high at P/N ratio of 1/15 and 1/30, but decreased significantly when the ratio changed to 1/45 and 1/50

($p<0.001$). High polymer content prevented the ethidium bromide from binding to pDNA and facilitated condensation. Therefore, we applied P/N at 1/50 for vaccine condensation and *in vivo* studies.

High nitric oxide was released in DC 2.4 cells after treatment with adjuvanted pDNA nanoparticulate vaccine

Nitric oxide (NO) is an important marker of innate immune response, and is released by DC 2.4 cells after antigen uptake and processing. The pDNA nanoparticulate vaccine (pDNA NP Vac) induced a higher amount of nitrite than the naked pDNA [8]. Here, we further assessed the efficacy of adjuvanted pDNA nanoparticulate vaccine (pDNA NP+Adj) to produce nitrite. Figure 2 demonstrated 16 hr and 24 hr after vaccine pulse/stimulation, that the nitrite produced was significantly higher in the adjuvanted group relative to pDNA ($p<0.001$) and pDNA NP Vac ($p<0.01$). Thus, we expect our pDNA NP+Adj would induce a strong antibody response in mice. Co-administration of Alum and antigen may cause the antigen to release slowly from the surface of Alum, resulting in an increased retention at the site of administration, thereby enhancing its cellular uptake by antigen-presenting cells [42]. Adjuvant MF59 may work *via* depot effect or by inducing monocyte to DC differentiation, creating an 'immunocompetent environment' at the injection site [43].

Adjuvanted pDNA nanoparticulate vaccine induced high and balanced MHC I & MHC II expression

We assessed the expression of MHC I and MHC II molecules on the surface of DCs pulsed individually with pDNA, pDNA NP Vac, and pDNA NP+Adj. Figure 3 showed the mean fluorescence intensity (MFI) ratios of MHC I and MHC II molecules were higher in the nanoparticulate group than soluble pDNA vaccine ($p<0.05$). Addition of adjuvants to pDNA nanoparticulate vaccine further enhanced the expression of both MHC I and MHC II molecules compared to pDNA vaccine (MHC I - $p<0.01$, MHC II - $p<0.001$). Overall, the expression of MHC 1 was higher than MHC II, but the adjuvanted vaccine resulted in a balanced MHC I and MHC II expressions.

Adjuvanted pDNA nanoparticulate vaccine induced long and stable anti-GnRH antibodies in mice

Mice were given a single dose of vaccine in all treatment groups. No GnRH-specific antibodies were detected in the control mice. In the pDNA group, measurable anti-GnRH IgG was detected on week 5 after immunization, maintained until week 12, with a slight decrease. In mice vaccinated with pDNA nanoparticulate vaccine with or without adjuvant, the GnRH antibodies were observed on week 3, peaked on week 9, and maintained at a high level until week 12 (Figure 4). Overall, no significant GnRH antibody increase was observed until week 4 in all vaccinated mice. GnRH antibodies were higher in both the nanoparticulate vaccine and adjuvanted groups than the pDNA vaccine group on weeks 2, 3, and 4. The GnRH antibodies in the adjuvanted group were always significantly higher than the non-adjuvanted group (Week 5-9: $p<0.01$, pDNA NP vaccine; $p<0.001$, pDNA vaccine; week 9-12: $p<0.001$, pDNA NP vaccine). After week 12, all mice were sacrificed, and spleens and lymph nodes were collected for further studies.

Adjuvanted pDNA nanoparticulate vaccine induced a Th2 immune response in mice

We used the peak serum on week 10 after immunization for IgG subclass characterization. In Figure 5, both IgG2a and IgG1 were increased when pDNA vaccine was formulated into either nanoparticles or nanoparticles plus adjuvants. That the IgG2a/IgG1 ratio >1 in the pDNA and pDNA NP Vac suggests a cell-mediated Th1 immune response. Supplementation of pDNA NP Vac with adjuvants significantly enhanced the IgG2a ($p<0.05$) and IgG1 ($p<0.01$), and resulted in a mixed Th1/Th2 response (Figure 5A and B). On week 10, the ratio of IgG2a/IgG1 <1 indicated a dominant humoral immune response and confirmed the use of adjuvants polarized the immune response towards Th2, characterized by high IgG1 expression.

Antibody avidity was increased after administration of adjuvanted pDNA nanoparticulate vaccine in mice

High avidity antibodies are capable of responding to low levels of cognate antigen after vaccination. In Figure 6, the AI on week 3 was 0.1M for pDNA, and 0.3M for both pDNA NP Vac and pDNA NP+Adj. The AI increased over time after immunization, reaching 0.3M for pDNA, 0.5M for pDNA NP Vac, and 0.7 for pDNA NP+Adj when the mice were euthanized on week 12.

Adjuvanated pDNA nanoparticulate vaccine enhanced lymphocyte proliferation in vitro

Splenocytes were harvested from mice 12 weeks after completion of immunization, and re-stimulated *in vitro* using the formulated vaccines. Figure 7 showed significantly higher stimulation index in the pDNA NP+Adj in comparison to pDNA ($p<0.01$), and pDNA NP Vac ($p<0.05$), indicating the presence of adjuvants and the nanoparticulate form of vaccine provided additional stimulus for lymphocyte proliferation.

T cells, B cells, but not memory B cells, were increased after re-stimulation by the adjuvanted pDNA nanoparticulate vaccine

The splenocytes and lymphnodes in mice were harvested for cultivation 12 weeks after completion of immunization, and re-stimulated *in vitro* with formulated vaccines.

In splenocytes, the $CD8^+$ T cells increased slightly in comparison to pDNA, from 2.1 % to 3.0 % for pDNA NP Vac ($p<0.05$), and from 2.1% to 3.6% for pDNA NP+Adj ($p<0.05$) (Figure 8). The expression of CD62L in $CD8^+$ T cells did not change (data not shown). For B cells using the CD45R marker, 46.8% of splenocytes were positive for pDNA, 55.9% for pDNA NP Vac ($p<0.05$), and 65.4% for pDNA NP+Adj ($p<0.001$) (Figure 9). The change of memory B cells was negligible (data not shown).

In lymph nodes, $CD8^+$ cells was increased markedly in comparison to pDNA, from 11.8% to 13.6% for pDNA NP Vac ($p<0.001$), and from 11.8% to 21.7% for pDNA NP+Adj ($p<0.001$) (Figure 8B). CD62L in $CD8^+$ cells was increased only in the adjuvanted group. For B cells, 62.1% of splenocytes were positive for pDNA, 81.5% for pDNA NP Vac ($p<0.01$), and 86.3% for pDNA NP+Adj ($p<0.001$) (Figure 9B). Memory B cells did not change significantly.

The adjuvanted pDNA nanoparticulate vaccine induced high expression of IL-4, suggesting a Th2 cytokine expression

Splenocytes were harvested from the immunized mice for *in vitro* stimulation, and IL-4 and IFN-ϒ expression were analyzed via flow cytometry. In Figure 10A, IFN-ϒ was increased, but was marginal when comparing the adjuvanted vaccine to the pDNA NP Vac, suggesting a Th1 polarized cytokine expression profile. In Figure 10B, IL-4 was significantly higher in pDNA NP+Adj vaccination than the non-adjuvanted vaccinations ($p<0.01$, pDNA Vac; $p<0.001$, pDNA NP Vac), indicating a Th2 polarized cytokine expression profile.

DISCUSSION

The pDNA vaccine is intended to induce both immunocontraception and rabies protection in animals. The success of using pDNA for rabies vaccination has been published [8, 13, 14], and here we focused on evaluating GnRH responses. To achieve immunocontraception is challenging, and there has been limited progress to date, with GonaCon™ (a GnRH based vaccine) licensed conditionally by EPA for deer [22][44][45]. We formulated an adjuvanted particulate pDNA vaccine in poloxamer gel (pDNA NP+Adj) to improve vaccine release and presentation to immune cells.

Anti-GnRH antibodies capture and neutralize GnRH release from the hypothalamus, thus preventing GnRH from binding to the receptors on pituitary gland and interfering with release of FSH and LH from the anterior pituitary gland. The cascade effect impacts maturation of ovarian follicles or spermatogenesis to achieve immunocontraception.

To improve vaccine immunization, an effective innate immune response and antigen presentation are crucial. Prior to *in vivo* studies, we assessed the vaccines in DC 2.4 cells, and found pDNA NP+Adj induced high nitric oxide and enhanced expression of MHC I and MHC II. The pDNA vaccine alone generated a Th1 biased MHC I response. The particulate pDNA vaccine and the addition of adjuvants greatly enhanced the expression of MHC II, resulting in a balanced MHC I and MHC II response.

Adjuvants Alum and MF 59 have been used for decades to increase the efficacy of vaccines by potentiating the humoral immune response. Alum is known to induce a Th 2 dependent immune response mediated by induction of reactive oxygen species release and activation of NLRP3 inflammasome in antigen presenting cells [51]. MF59 is NLRP3 independent and generates a robust innate immune response at the site of vaccination [52]. MF59 also enhances a cross-reactive immune response and generates a strong immune memory to maintain long-lasting humoral immunity.

Chitosan is known to enable endosomal escape of nanoparticulate vaccine via a ‘proton sponge effect’, similar to polyethyleneimine (PEI) [46]. Chitosan also could exhibit adjuvant effects by stimulating the innate immune response [47] [48]. In the current study, we adsorbed the pDNA on the surface of PLGA-chitosan nanoparticles to prevent the vaccine from undergoing harsh processing conditions of high temperature and exposure to organic solvents. Previous studies have found pDNA in organic solvents either aggregates or exists

as P form which is devoid of stacking interactions and hydrogen bonding resulting in denaturation of pDNA [49] [50].

In our mice study, the pDNA NP+Adj induced high GnRH antibodies, and maintained the high titer up to 12 weeks after immunization when the animal experiment was terminated. This improvement could be attributed to antigen slow release in the poloxamer gel, and/or the nanoparticulate form of antigen increasing antigen presentation and cellular uptake.

Administration of particulate vaccine dispersed in thermosensitive gel forms a depot at the site of vaccination and thereby enhances its retention time and prevents the distribution of vaccine particulates to other parts of body [53] [54]. Consequently, more antigenic particles became available for cellular uptake by local muscle cells and resident DCs.

Avidity index indicates binding strength between antigen and antibody, and antibody avidity generally correlates well with functional activity. Antigens in low concentration are going to be recognized by antibodies with high avidity index. In the animal study, we observed the avidity index for GnRH antibodies was increased after immunization using pDNA NP+Adj, and maintained for up to 12 weeks. Since GnRH is a self-antigen in low qunatity in the body, high avidity anti-GnRH antibodies will have a better chance to capture the cognate antigen.

In our previous study, the pDNA vaccine alone induced a Th1-biased response; cellular immune dominated [8]. However, for immunocontraception using GnRH as a target, antibodies play a major role. We intended to skew the immune reponse toward a balanced Th1/Th2 using a novel vaccine formuation. Indeed, after immunization of mice using pDNA NP+Adj, we detected a significantly enhanced expression of IgG1 over IgG2a, with the ratio of IgG2a/IgG1 <1, indicating a polarized Th2 humoral immune response. By cytokine analysis, we also observed a high expression of IL-4 over IFN-γ in the pDNA NP+Adj immunized mice, suggesting a Th2 cytokine expression profile. Both T and B cell proliferation were increased, but immune memory did not change much in the new vaccine formulation. We anticipate the slow release of antigen encapsulated in the gel will be a surrogate for immune memory in inducing long and lasting humoral responses for immunocontraception and rabies protection.

CONCLUSION

Our results demonstrated the a pDNA nanoparticulate vaccine dispersed in hydrogel generates both humoral and cell-mediated immune responses. The antibody response was further potentiated using the adjuvants in the particulate vaccine, skewing the Th1/Th2 immune profile toward Th2, thus favoring antibody production. The enhanced immune response could be attributed to the increased cellular uptake of particulate vaccine over the soluble form of pDNA. The poloxamer gel provide an increased retention of particulate vaccine at the vaccination site for long immune stimulus. Our pDNA NP+Adj is a Th2 dominant vaccine for generating GnRH antibodies and protection against rabies. Future evaluations will determine the effectiveness of this novel dual immunocontraception and rabies vaccine to provide protection from rabies challenge and sterility within the animal.

Acknowledgements

The authors would acknowledge the use of facilities of Vaccine Nanotechnology Laboratory, Department of Pharmaceutical Sciences, College of Pharmacy and Health Sciences, Mercer University, Atlanta, GA. The results of the study will be a part of Amit Bansal's dissertation.

The findings and conclusions in this report are those of the authors and do not necessarily represent the views of the Centers for Disease Control and Prevention.

Funding

This research did not receive any specific funding from agencies in the public, commercial, or not-for-profit sectors.

References

[1]. Wilde H, Ghai S, Hemachudha T, Rabies: Still a silent killer targeting the poor, Vaccine. 35 (2017) 2293–2294. doi:10.1016/j.vaccine.2017.03.001. [PubMed: 28343778]

[2]. Wilde H, Lumlertdacha B, Meslin FX, Ghai S, Hemachudha T, Worldwide rabies deaths prevention--A focus on the current inadequacies in postexposure prophylaxis of animal bite victims, Vaccine. 34 (2016) 187–189. doi:10.1016/j.vaccine.2015.11.036. [PubMed: 26626211]

[3]. Bose A, Munshi R, Tripathy RM, Madhusudana SN, Harish BR, Thaker S, Mahendra BJ, Gunale B, Gogtay NJ, Thatte UM, Mani RS, Manjunath K, George K, Yajaman AB, Sahai A, Dhere RM, Alex RG, Adhikari DD, Abhilash null, Raghava V, Kumbhar D, Behera TR, Kulkarni PS, A randomized non-inferiority clinical study to assess post-exposure prophylaxis by a new purified vero cell rabies vaccine (Rabivax-S) administered by intramuscular and intradermal routes, Vaccine. 34 (2016) 4820–4826. doi:10.1016/j.vaccine.2016.08.005. [PubMed: 27554534]

[4]. Arya JM, Dewitt K, Scott-Garrard M, Chiang Y-W, Prausnitz MR, Rabies vaccination in dogs using a dissolving microneedle patch, Journal of Controlled Release. 239 (2016) 19–26. doi:10.1016/j.jconrel.2016.08.012. [PubMed: 27524283]

[5]. Dürr S, Fahrion AS, Knopf L, Taylor LH, Editorial: Towards Elimination of Dog Mediated Human Rabies, Front Vet Sci. 4 (2017). doi:10.3389/fvets.2017.00142.

[6]. Alliance for Contraception in Cats & Dogs (ACC&D), Immunocontraceptive Approaches for Sterilization of Dogs and Cats, Scientic Think Tank, in: Roanoke, VA, 2009.

[7]. Herbert M, Riyaz Basha S, Thangaraj S, Community perception regarding rabies prevention and stray dog control in urban slums in India, J Infect Public Health. 5 (2012) 374–380. doi:10.1016/j.jiph.2012.05.002. [PubMed: 23287607]

[8]. Bansal A, Wu X, Olson V, D'Souza MJ, Characterization of rabies pDNA nanoparticulate vaccine in poloxamer 407 gel, Int J Pharm. 545 (2018) 318–328. doi:10.1016/j.ijpharm.2018.05.018. [PubMed: 29746999]

[9]. Millar RP, GnRHs and GnRH receptors, Anim. Reprod. Sci. 88 (2005) 5–28. doi:10.1016/j.anireprosci.2005.05.032. [PubMed: 16140177]

[10]. Sharma S, McDonald I, Miller L, Hinds LA, Parenteral administration of GnRH constructs and adjuvants: immune responses and effects on reproductive tissues of male mice, Vaccine. 32 (2014) 5555–5563. doi:10.1016/j.vaccine.2014.07.075. [PubMed: 25130539]

[11]. Ladd A, Progress in the development of anti-LHRH vaccine, Am. J. Reprod. Immunol. 29 (1993) 189–194. [PubMed: 8373528]

[12]. Fagerstone KA, Miller LA, Killian G, Yoder CA, Review of issues concerning the use of reproductive inhibitors, with particular emphasis on resolving human-wildlife conflicts in North America, Integr Zool. 5 (2010) 15–30. doi:10.1111/j.1749-4877.2010.00185.x. [PubMed: 21392318]

[13]. Wu X, Franka R, Svoboda P, Pohl J, Rupprecht CE, Development of combined vaccines for rabies and immunocontraception, Vaccine. 27 (2009) 7202–7209. doi:10.1016/j.vaccine.2009.09.025. [PubMed: 19925954]

[14]. Wu X, Smith TG, Franka R, Wang M, Carson WC, Rupprecht CE, The feasibility of rabies virus-vectored immunocontraception in a mouse model, Trials in Vaccinology. 3 (2014) 11–18. doi:10.1016/j.trivac.2013.11.003.

[15]. Billeskov R, Wang Y, Solaymani-Mohammadi S, Frey B, Kulkarni S, Andersen P, Agger EM, Sui Y, Berzofsky JA, Low Antigen Dose in Adjuvant-Based Vaccination Selectively Induces CD4 T Cells with Enhanced Functional Avidity and Protective Efficacy, J Immunol. 198 (2017) 3494–3506. doi:10.4049/jimmunol.1600965. [PubMed: 28348274]

[16]. Pedersen GK, Höschler K, Øie Solbak SM, Bredholt G, Pathirana RD, Afsar A, Breakwell L, Nøstbakken JK, Raae AJ, Brokstad KA, Sjursen H, Zambon M, Cox RJ, Serum IgG titres, but not avidity, correlates with neutralizing antibody response after H5N1 vaccination, Vaccine. 32 (2014) 4550–4557. doi:10.1016/j.vaccine.2014.06.009. [PubMed: 24950357]

[17]. Usinger WR, Lucas AH, Avidity as a determinant of the protective efficacy of human antibodies to pneumococcal capsular polysaccharides, Infect. Immun. 67 (1999) 2366–2370. [PubMed: 10225896]

[18]. Breukels MA, Jol-van der Zijde E, van Tol MJD, Rijkers GT, Concentration and avidity of anti-Haemophilus influenzae type b (Hib) antibodies in serum samples obtained from patients for whom Hib vaccination failed, Clin. Infect. Dis. 34 (2002) 191–197. doi:10.1086/338259. [PubMed: 11740707]

[19]. Scheerlinck J-PY, Greenwood DLV, Particulate delivery systems for animal vaccines, Methods. 40 (2006) 118–124. doi:10.1016/j.ymeth.2006.05.023. [PubMed: 16997719]

[20]. Samoylov A, Cochran A, Schemera B, Kutzler M, Donovan C, Petrenko V, Bartol F, Samoylova T, Humoral immune responses against gonadotropin releasing hormone elicited by immunization with phage-peptide constructs obtained via phage display, J. Biotechnol. 216 (2015) 20–28. doi:10.1016/j.jbiotec.2015.10.001. [PubMed: 26456116]

[21]. Xu J, Zhu Z, Wu J, Liu W, Shen X, Zhang Y, Hu Z, Zhu D, Roque RS, Liu J, Immunization with a recombinant GnRH vaccine conjugated to heat shock protein 65 inhibits tumor growth in orthotopic prostate cancer mouse model, Cancer Lett. 259 (2008) 240–250. doi:10.1016/j.canlet.2007.10.011. [PubMed: 18039558]

[22]. Miller LA, Gionfriddo JP, Fagerstone KA, Rhyan JC, Killian GJ, The single-shot GnRH immunocontraceptive vaccine (GonaCon) in white-tailed deer: comparison of several GnRH preparations, Am. J. Reprod. Immunol. 60 (2008) 214–223. doi:10.1111/j.1600-0897.2008.00616.x. [PubMed: 18782282]

[23]. Jung M-J, Moon Y-C, Cho I-H, Yeh J-Y, Kim S-E, Chang W-S, Park S-Y, Song C-S, Kim H-Y, Park K-K, McOrist S, Choi I-S, Lee J-B, Induction of castration by immunization of male dogs with recombinant gonadotropin-releasing hormone (GnRH)-canine distemper virus (CDV) T helper cell epitope p35, J. Vet. Sci. 6 (2005) 21–24. [PubMed: 15785119]

[24]. Hem SL, Hogenesch H, Relationship between physical and chemical properties of aluminum-containing adjuvants and immunopotentiation, Expert Rev Vaccines. 6 (2007) 685–698. doi:10.1586/14760584.6.5.685. [PubMed: 17931150]

[25]. Garg R, Kaur M, Saxena A, Prasad R, Bhatnagar R, Alum adjuvanted rabies DNA vaccine confers 80% protection against lethal 50 LD50 rabies challenge virus standard strain, Molecular Immunology. 85 (2017) 166–173. doi:10.1016/j.molimm.2017.02.011. [PubMed: 28267643]

[26]. Xu J, Zhu Z, Duan P, Li W, Zhang Y, Wu J, Hu Z, Roque RS, Liu J, Cloning, expression, and purification of a highly immunogenic recombinant gonadotropin-releasing hormone (GnRH) chimeric peptide, Protein Expr. Purif. 50 (2006) 163–170. doi:10.1016/j.pep.2006.08.016. [PubMed: 17064933]

[27]. Taetz S, Nafee N, Beisner J, Piotrowska K, Baldes C, Mürdter TE, Huwer H, Schneider M, Schaefer UF, Klotz U, Lehr C-M, The influence of chitosan content in cationic chitosan/PLGA nanoparticles on the delivery efficiency of antisense 2'-O-methyl-RNA directed against telomerase in lung cancer cells, Eur J Pharm Biopharm. 72 (2009) 358–369. doi:10.1016/j.ejpb.2008.07.011. [PubMed: 18703137]

[28]. Najafi H, Abolmaali SS, Owrangi B, Ghasemi Y, Tamaddon AM, Serum resistant and enhanced transfection of plasmid DNA by PEG-stabilized polyplex nanoparticles of L-histidine substituted polyethyleneimine, Macromol. Res. 23 (2015) 618–627. doi:10.1007/s13233-015-3074-5.

[29]. Rezvani Amin Z, Rahimizadeh M, Eshghi H, Dehshahri A, Ramezani M, The effect of cationic charge density change on transfection efficiency of polyethylenimine, Iran J Basic Med Sci. 16 (2013) 150–156. [PubMed: 24298383]

[30]. Eastman SJ, Siegel C, Tousignant J, Smith AE, Cheng SH, Scheule RK, Biophysical characterization of cationic lipid: DNA complexes, Biochim. Biophys. Acta. 1325 (1997) 41–62. [PubMed: 9106482]

[31]. Chae SY, Lee M, Kim SW, Bae YH, Protection of insulin secreting cells from nitric oxide induced cellular damage by crosslinked hemoglobin, Biomaterials. 25 (2004) 843–850. [PubMed: 14609673]

[32]. Bogdan C, Röllinghoff M, Diefenbach A, The role of nitric oxide in innate immunity, Immunol. Rev. 173 (2000) 17–26. [PubMed: 10719664]

[33]. Jinshu X, Jingjing L, Duan P, Zheng Z, Ding M, Jie W, Rongyue C, Zhuoyi H, Roque RS, A synthetic gonadotropin-releasing hormone (GnRH) vaccine for control of fertility and hormone dependent diseases without any adjuvant, Vaccine. 23 (2005) 4834–4843. doi:10.1016/j.vaccine.2005.05.010. [PubMed: 15996796]

[34]. Ghosh S, Jackson DC, Antigenic and immunogenic properties of totally synthetic peptide-based anti-fertility vaccines, Int. Immunol. 11 (1999) 1103–1110. [PubMed: 10383943]

[35]. Romero-Steiner S, Musher DM, Cetron MS, Pais LB, Groover JE, Fiore AE, Plikaytis BD, Carlone GM, Reduction in functional antibody activity against Streptococcus pneumoniae in vaccinated elderly individuals highly correlates with decreased IgG antibody avidity, Clin. Infect. Dis. 29 (1999) 281–288. doi:10.1086/520200. [PubMed: 10476727]

[36]. Chen B-Y, Zhou G, Li Q-L, Lu J-S, Shi D-Y, Pang X-B, Zhou X-W, Yu Y-Z, Huang P-T, Enhanced effects of DNA vaccine against botulinum neurotoxin serotype A by targeting antigen to dendritic cells, Immunol. Lett. 190 (2017) 118–124. doi:10.1016/j.imlet.2017.08.004. [PubMed: 28802641]

[37]. Tawde SA, Chablani L, Akalkotkar A, D'Souza MJ, Evaluation of microparticulate ovarian cancer vaccine via transdermal route of delivery, J Control Release. 235 (2016) 147–154. doi:10.1016/j.jconrel.2016.05.058. [PubMed: 27238440]

[38]. Caraher EM, Parenteau M, Gruber H, Scott FW, Flow cytometric analysis of intracellular IFN-gamma, IL-4 and IL-10 in CD3(+)4(+) T-cells from rat spleen, J. Immunol. Methods. 244 (2000) 29–40. [PubMed: 11033016]

[39]. Pala P, Hussell T, Openshaw PJ, Flow cytometric measurement of intracellular cytokines, J. Immunol. Methods. 243 (2000) 107–124. [PubMed: 10986410]

[40]. Agarwal R, Roy K, Intracellular delivery of polymeric nanocarriers: a matter of size, shape, charge, elasticity and surface composition, Ther Deliv. 4 (2013) 705–723. doi:10.4155/tde.13.37. [PubMed: 23738668]

[41]. Agarwal R, Singh V, Jurney P, Shi L, Sreenivasan SV, Roy K, Scalable imprinting of shape-specific polymeric nanocarriers using a release layer of switchable water solubility, ACS Nano. 6 (2012) 2524–2531. doi:10.1021/nn2049152. [PubMed: 22385068]

[42]. Morefield GL, Sokolovska A, Jiang D, HogenEsch H, Robinson JP, Hem SL, Role of aluminum-containing adjuvants in antigen internalization by dendritic cells in vitro, Vaccine. 23 (2005) 1588–1595. doi:10.1016/j.vaccine.2004.07.050. [PubMed: 15694511]

[43]. O'Hagan DT, Ott GS, De Gregorio E, Seubert A, The mechanism of action of MF59 - an innately attractive adjuvant formulation, Vaccine. 30 (2012) 4341–4348. doi:10.1016/j.vaccine.2011.09.061. [PubMed: 22682289]

[44]. Killian G, Kreeger TJ, Rhyan J, Fagerstone K, Miller L, Observations on the use of GonaCon in captive female elk (Cervus elaphus), J. Wildl. Dis. 45 (2009) 184–188. doi:10.7589/0090-3558-45.1.184. [PubMed: 19204347]

[45]. Vargas-Pino F, Gutiérrez-Cedillo V, Canales-Vargas EJ, Gress-Ortega LR, Miller LA, Rupprecht CE, Bender SC, García-Reyna P, Ocampo-López J, Slate D, Concomitant administration of GonaConTM and rabies vaccine in female dogs (Canis familiaris) in Mexico, Vaccine. 31 (2013) 4442–4447. doi:10.1016/j.vaccine.2013.06.061. [PubMed: 23871822]

[46]. Richard I, Thibault M, De Crescenzo G, Buschmann MD, Lavertu M, Ionization behavior of chitosan and chitosan-DNA polyplexes indicate that chitosan has a similar capability to

induce a proton-sponge effect as PEI, Biomacromolecules. 14 (2013) 1732–1740. doi:10.1021/bm4000713. [PubMed: 23675916]

[47]. Reddy ST, van der Vlies AJ, Simeoni E, Angeli V, Randolph GJ, O'Neil CP, Lee LK, Swartz MA, Hubbell JA, Exploiting lymphatic transport and complement activation in nanoparticle vaccines, Nat. Biotechnol. 25 (2007) 1159–1164. doi:10.1038/nbt1332. [PubMed: 17873867]

[48]. Dong X, Sun Z, Liang J, Wang H, Zhu D, Leng X, Wang C, Kong D, Lv F, A visible fluorescent nanovaccine based on functional genipin crosslinked ovalbumin protein nanoparticles, Nanomedicine. 14 (2018) 1087–1098. doi:10.1016/j.nano.2018.02.007. [PubMed: 29474923]

[49]. Bonner G, Klibanov AM, Structural stability of DNA in nonaqueous solvents, Biotechnol. Bioeng. 68 (2000) 339–344. [PubMed: 10745202]

[50]. Zehfus MH, Johnson WC, Conformation of P-form DNA, Biopolymers. 23 (1984) 1269–1281. doi:10.1002/bip.360230711. [PubMed: 6466767]

[51]. Ramanathan VD, Badenoch-Jones P, Turk JL, Complement activation by aluminium and zirconium compounds, Immunology. 37 (1979) 881–888. [PubMed: 500133]

[52]. Seubert A, Calabro S, Santini L, Galli B, Genovese A, Valentini S, Aprea S, Colaprico A, D'Oro U, Giuliani MM, Pallaoro M, Pizza M, O'Hagan DT, Wack A, Rappuoli R, De Gregorio E, Adjuvanticity of the oil-in-water emulsion MF59 is independent of Nlrp3 inflammasome but requires the adaptor protein MyD88, Proc. Natl. Acad. Sci. U.S.A. 108 (2011) 11169–11174. doi:10.1073/pnas.1107941108. [PubMed: 21690334]

[53]. Roques C, Salmon A, Fiszman MY, Fattal E, Fromes Y, Intrapericardial administration of novel DNA formulations based on thermosensitive Poloxamer 407 gel, International Journal of Pharmaceutics. 331 (2007) 220–223. doi:10.1016/j.ijpharm.2006.11.056. [PubMed: 17187948]

[54]. Kojarunchitt T, Baldursdottir S, Dong Y-D, Boyd BJ, Rades T, Hook S, Modified thermoresponsive Poloxamer 407 and chitosan sol–gels as potential sustained-release vaccine delivery systems, European Journal of Pharmaceutics and Biopharmaceutics. 89 (2015) 74–81. doi:10.1016/j.ejpb.2014.11.026. [PubMed: 25481034]

[55]. Alam MM, Arifuzzaman M, Ahmad SM, Hosen MI, Rahman MA, Rashu R, Sheikh A, Ryan ET, Calderwood SB, Qadri F, Study of avidity of antigen-specific antibody as a means of understanding development of long-term immunological memory after Vibrio cholerae O1 infection, Clin. Vaccine Immunol. 20 (2013) 17–23. doi:10.1128/CVI.00521-12. [PubMed: 23114701]

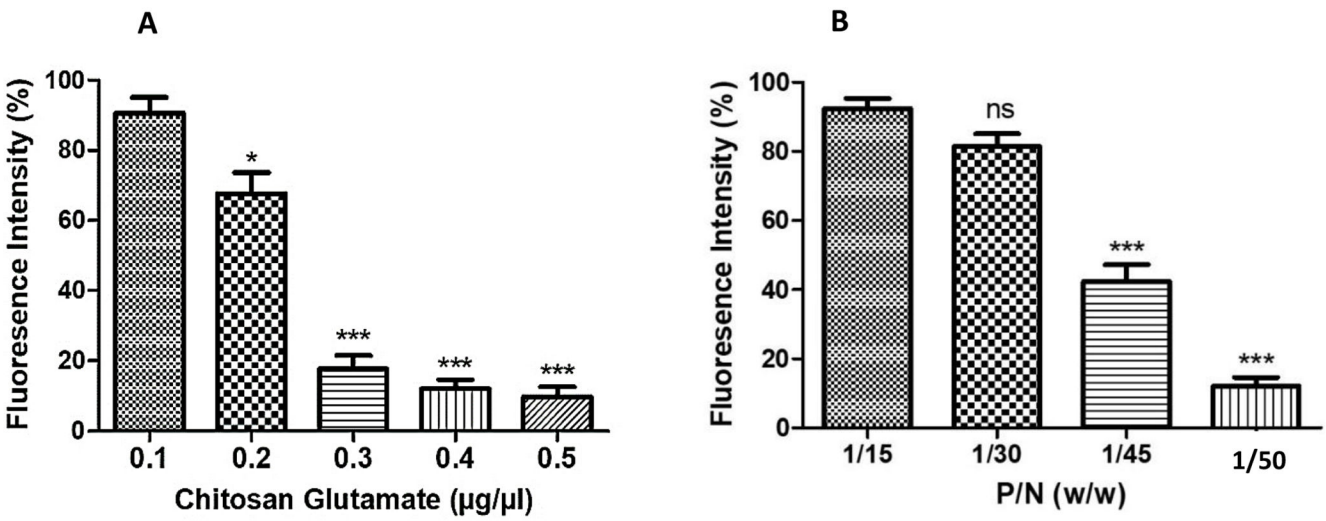

Figure 1 -

Ethidium bromide exclusion assay measuring the percent change in fluorescence intensity. (A) Percent decrease in fluorescence intensity was observed on addition of increasing concentrations of chitosan glutamate (0.1–0.5 µg/µL) and (B) percent decrease in fluorescence intensity with change in pDNA to nanoparticles ratio (P/N). ns - Not significant, *p<0.05 significant **p<0.01 very significant, ***p<0.001 extremely significant. Data are expressed as mean ± SEM.

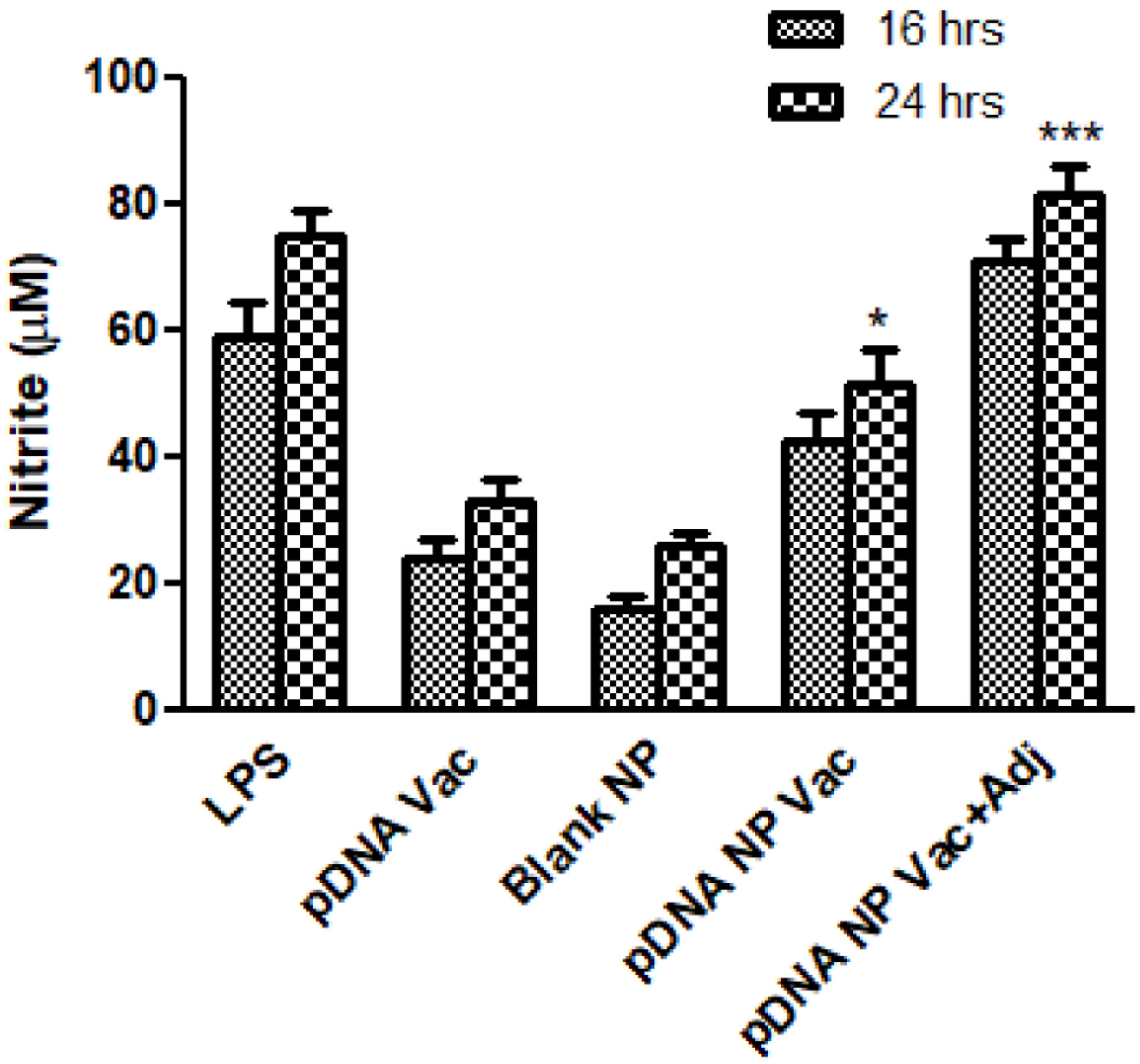

Figure 2 -

Nitrite release from DC 2.4 cells was measured by Griess assay. Murine DC 2.4 cells were pulsed with LPS (5 μg) as positive control, pDNA (1 μg), blank NP (50 μg), pDNA nanoparticulate vaccine (50 μg, pDNA amount 1 μg), and pDNA nanoparticulate vaccine plus adjuvants Alum and MF59. There was a significant increase in nitrite release by groups received pDNA nanoparticulate vaccine with or without adjuvant Alum and MF59 (*$p<0.05$ significant, **$p<0.01$very significant, ***$p<0.001$ extremely significant) measured using one-way ANOVA with Tukey post hoc test. Data are expressed as mean ± SEM.

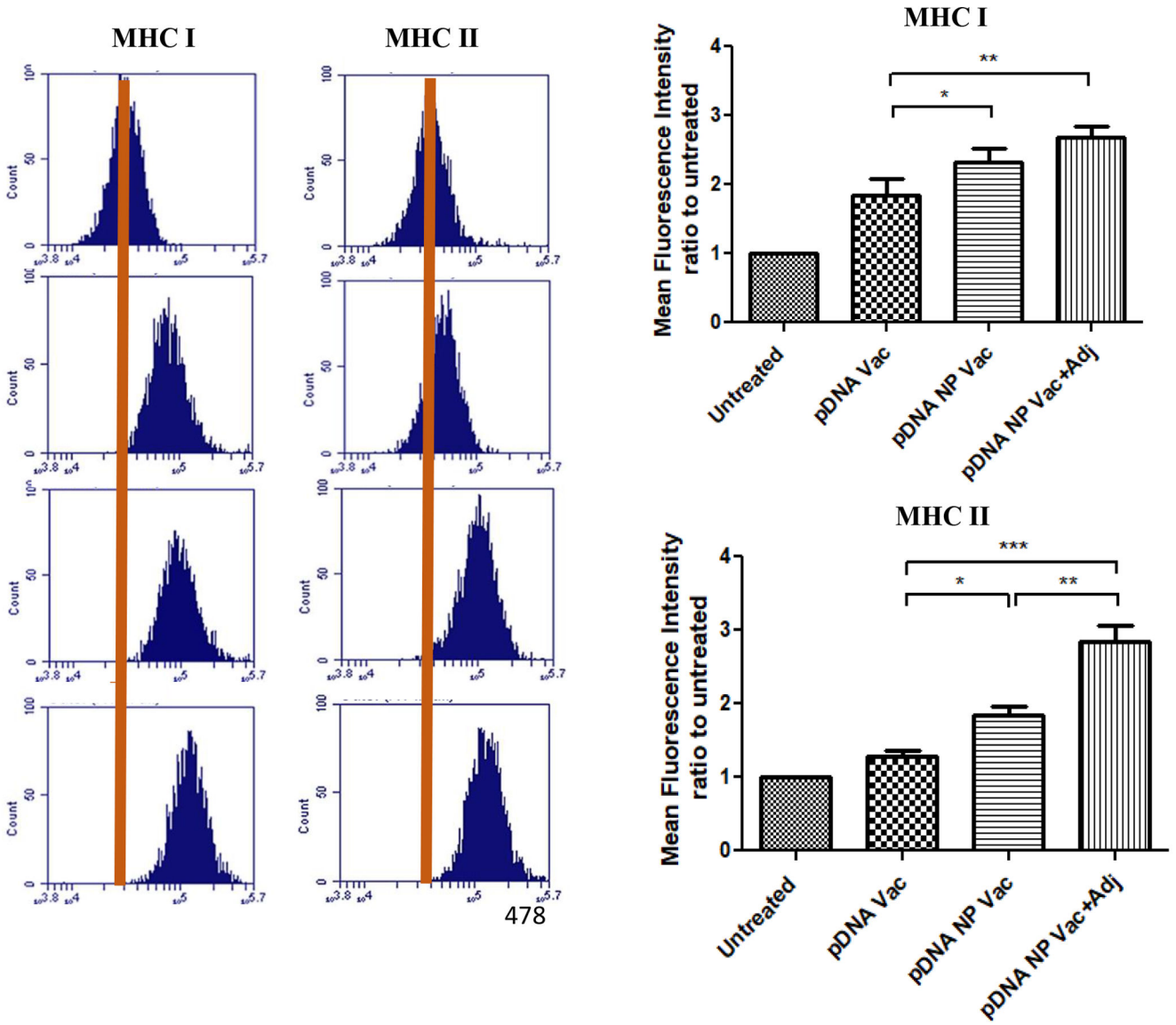

Figure 3 –.

Upregulation of maturation markers (i.e., MHC I and MHC II) on DCs post-exposure to various treatments. The expression of co-stimulatory molecules was detected by flow cytometry analysis of fluorescence-labelled CD80 and CD40 antibodies. DC 2.4 cells were exposed to an equivalent amount of pDNA in all treatment groups. Mean fluorescence intensity (MFI) ratios of treatment samples were plotted to untreated samples. Results were analyzed using one-way ANOVA followed by post hoc Tukey's multiple comparison test (*$p<0.05$ significant, **$p<0.01$ very significant, ***$p<0.001$ extremely significant). Data are expressed as mean±SEM, n=3, triplicate.

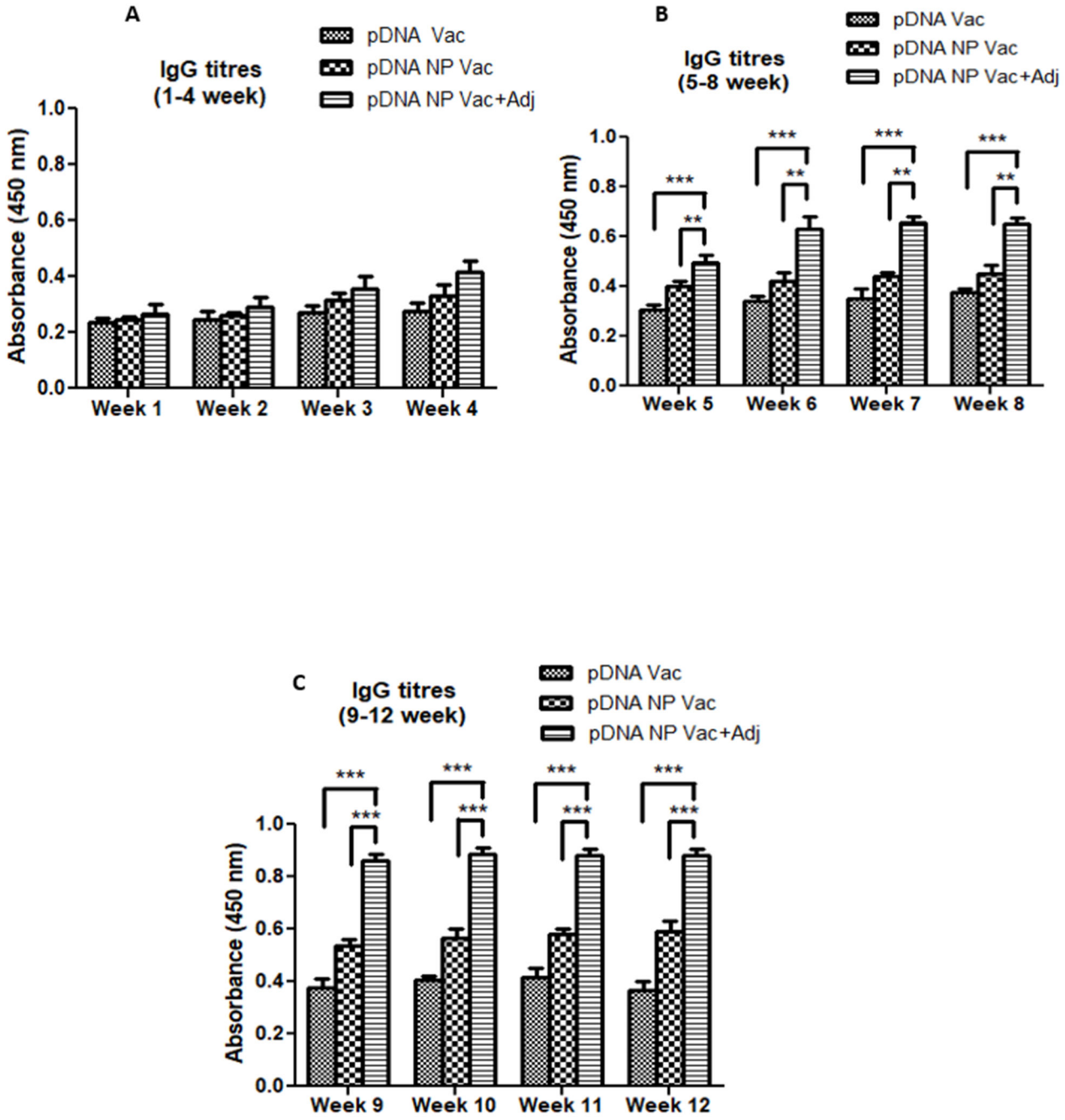

Figure 4 -

Antibody titers (IgG) in mice after rabies vaccination administered via intramuscular route (IM). Mice (n=6) were vaccinated on day 1 with pDNA (100 μg) in hydrogel, pDNA nanoparticulate vaccine in hydrogel, and pDNA nanoparticulate vaccine plus adjuvant in hydrogel. Blood was collected every week post-vaccination and analyzed for anti-GnRH antibodies using ELISA. Results were compared statistically among groups every week (*p<0.05 significant, **p<0.01very significant, ***p<0.001 extremely significant) using one-way ANOVA with Tukey post hoc test. Data are expressed as mean±SEM.

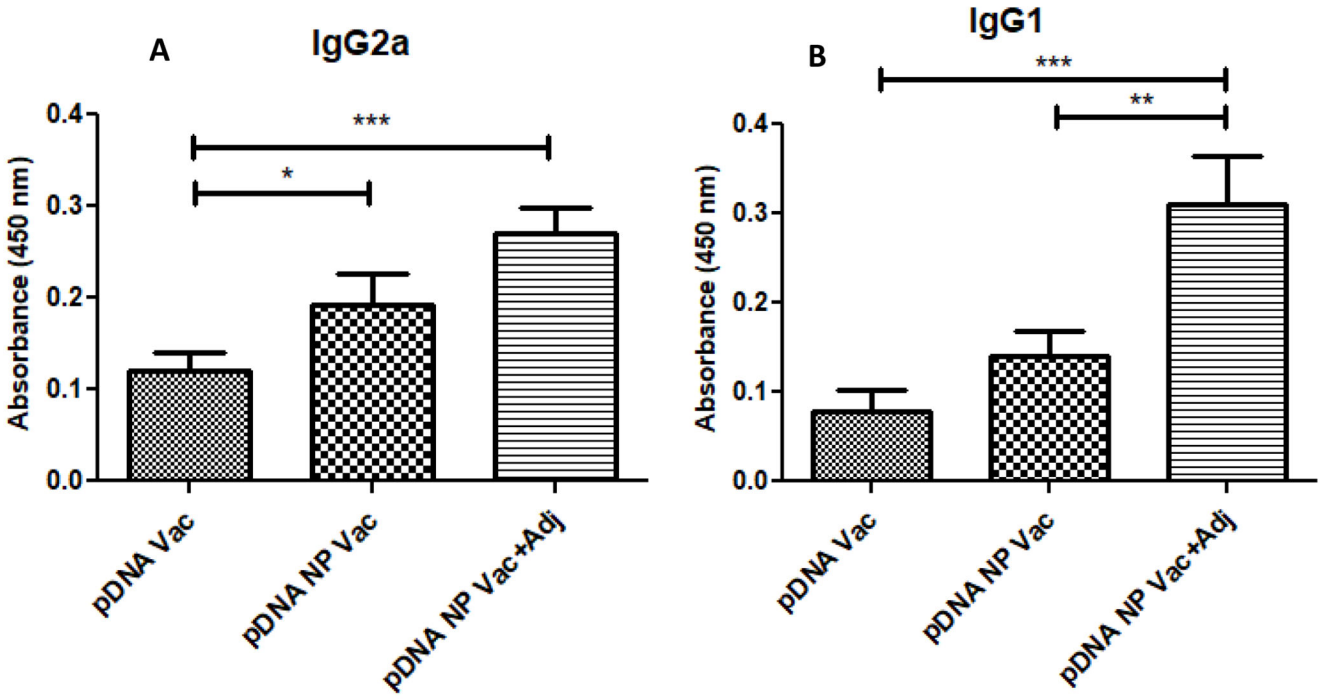

Figure 5 -

The anti-GnRH specific IgG subclass immune response. IgG subclass (IgG1, IgG2a) titers were measured in sera of mice (n=6) post vaccination on week 10. The IgG1/IgG2a ratio (ratios>1 and <1 indicate a Th2 and Th1 polarized response, respectively). A significant increase in titers was observed in pDNA nanoparticulate vaccine adjuvanted group (Alum and MF59). The p value was calculated (*p<0.05 significant, **p<0.01very significant, ***p<0.001 extremely significant) using one-way ANOVA with Tukey post hoc test. Data are expressed as mean ± SEM.

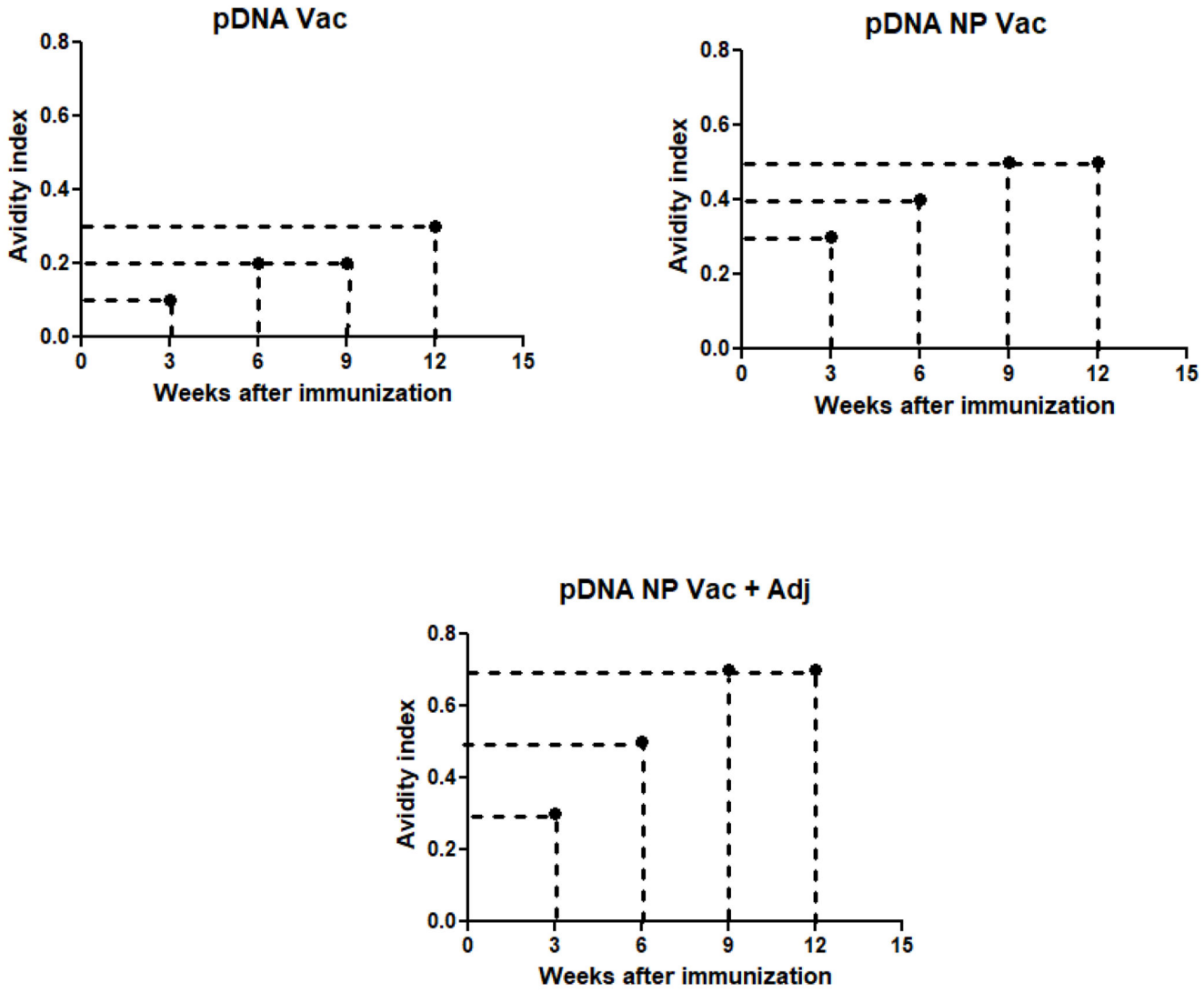

Figure 6 –.

Avidity index was determined by incubating serum with increasing concentrations of sodium thiocyanate and calculated as 50% reduction in absorbance from untreated samples. The three groups used for the study were pDNA vaccine (A), pDNA nanoparticulate vaccine (B) and pDNA nanoparticulate vaccine plus adjuvants (Alum and MF59) (C) and samples were measured for avidity index at weeks 3, 6, 9, and 12.

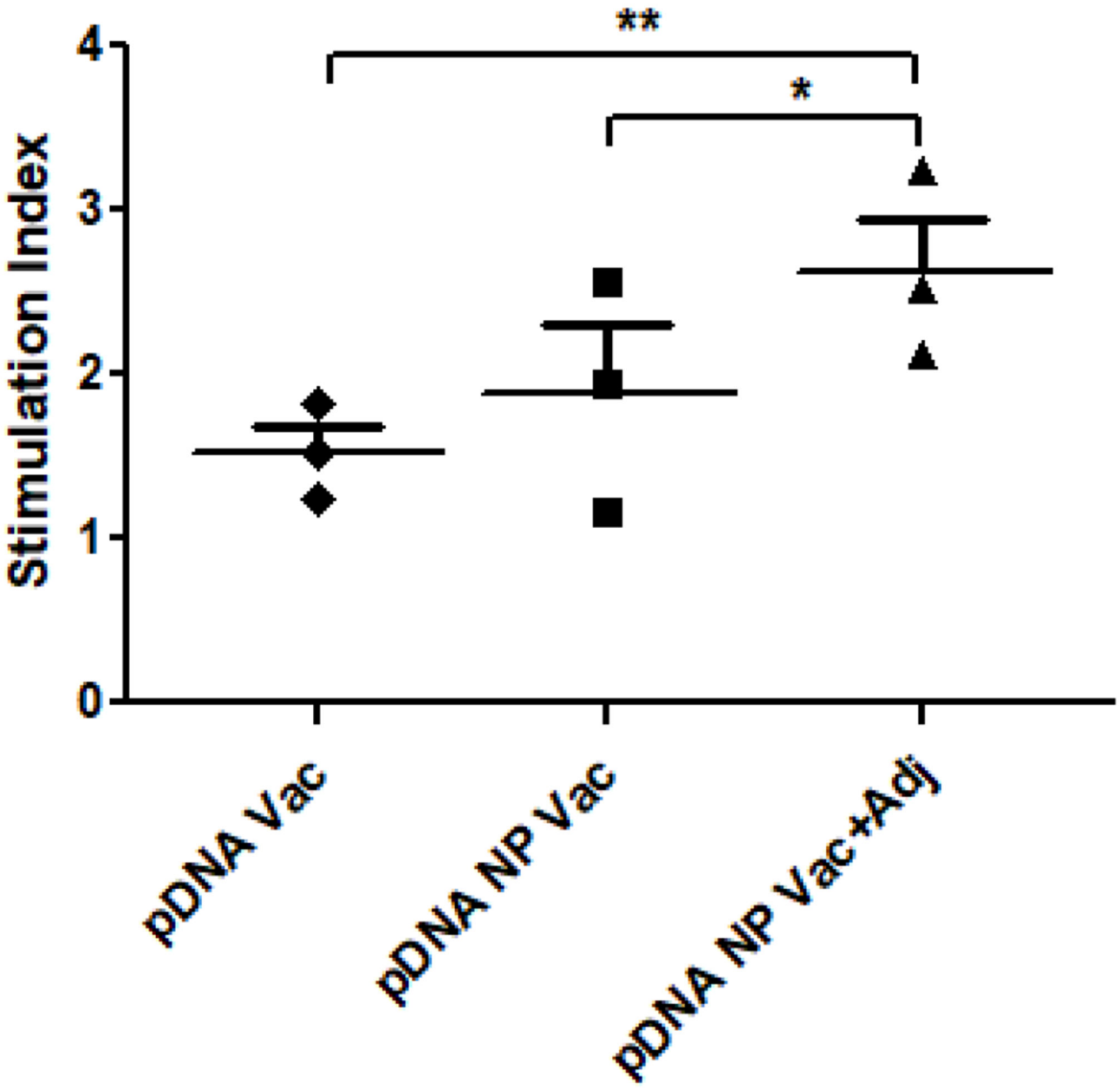

Figure 7 –.

In vitro proliferative response of splenocytes stimulated with different treatments was determined using alamar blue assay. The pDNA vaccine plus adjuvant group showed significantly higher stimulation over other treatment groups. The p value was calculated (*p<0.05 significant, **p<0.01 very significant, ***p<0.001 extremely significant) using one-way ANOVA with Tukey post hoc test. Data are expressed as mean ± SEM.

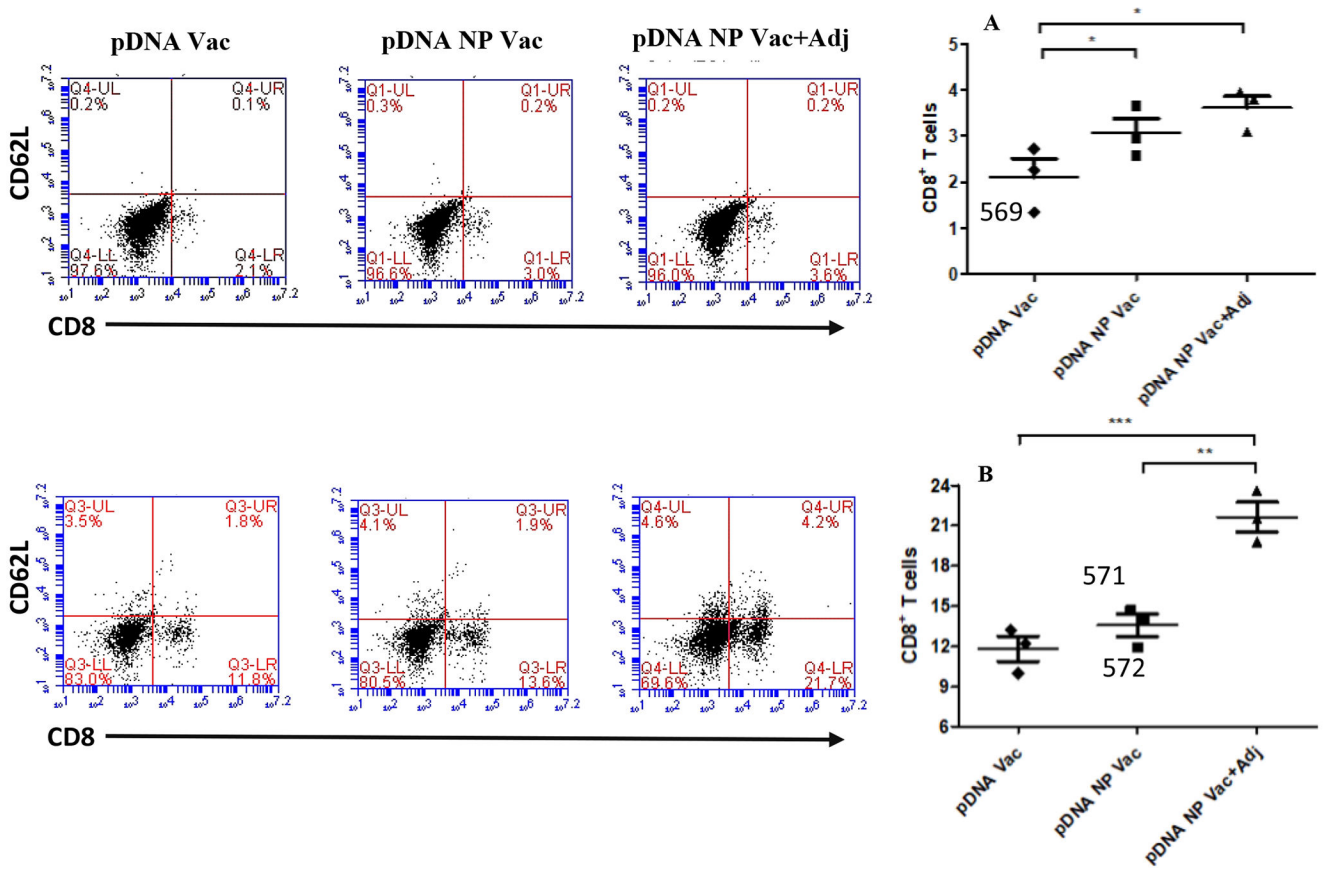

Figure 8 -

The activation of CD8 and CD62L positive cells in both splenocytes (top) and lymph node cells (bottom) were evaluated after re-stimulation with antigen. Representative flow cytometry dot plots for each group are shown in the figure above. Bar graphs plotted in figure 9A and B showed the CD8 positive cells in splenocytes and lymphnode cells. p value was calculated (*$p<0.05$ significant, **$p<0.01$ very significant, ***$p<0.001$ extremely significant) using one-way Anova, multiple comparison was performed using tukey's post hoc analysis. Data are expressed as mean ± SEM.

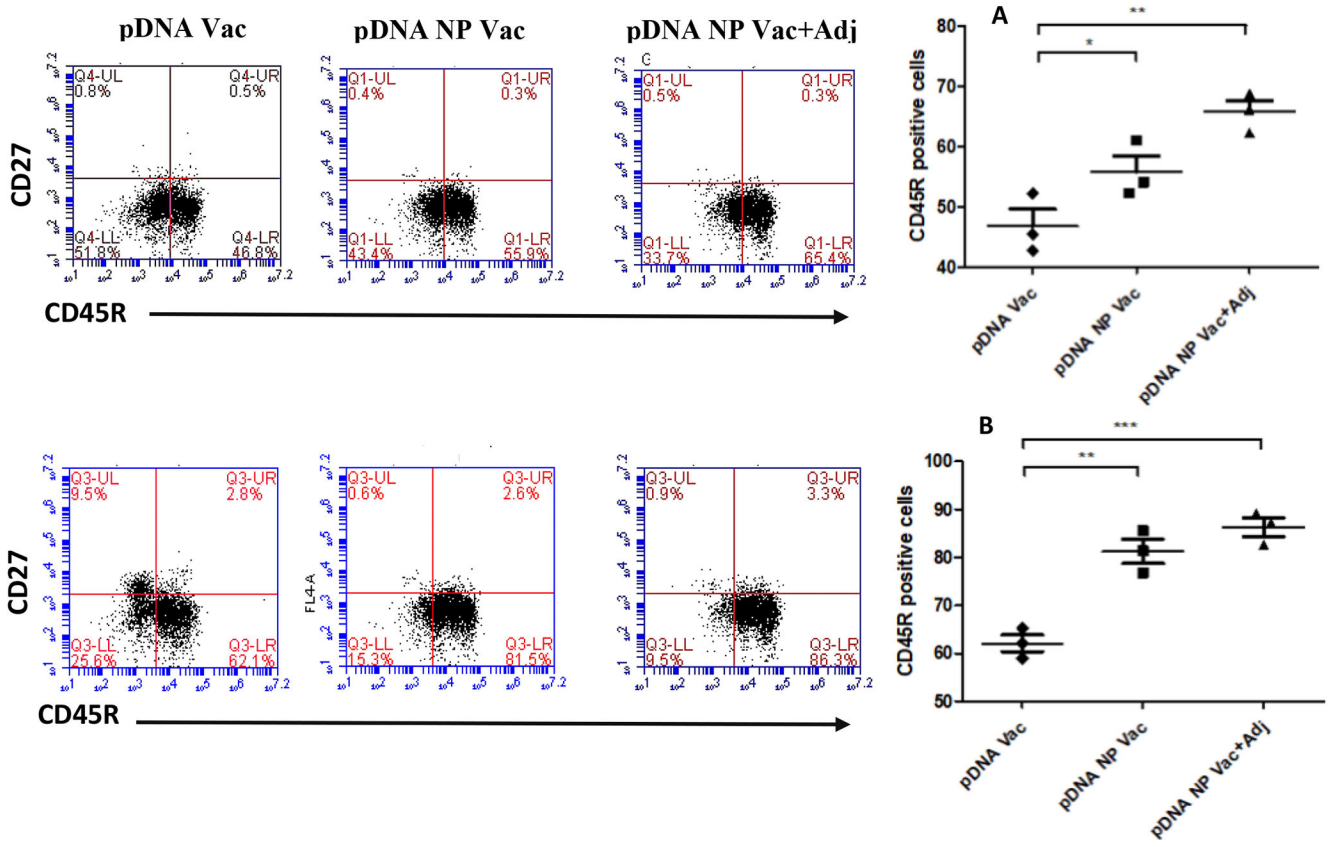

Figure 9 -

The activation of CD45R and CD27 positive cells in both splenocytes (top) and lymph node cells (bottom) were evaluated after re-stimulation with antigen. Representative flow cytometry dot plots for each group is shown in the figure above. Bar graphs plotted in figure 10A and B showed the CD45R positive cells in splenocytes and lymphnode cells. p value was calculated (*$p<0.05$ significant, **$p<0.01$ very significant, ***$p<0.001$ extremely significant) using one-way Anova, multiple comparison was performed using tukey's post hoc analysis. Data are expressed as mean ± SEM.

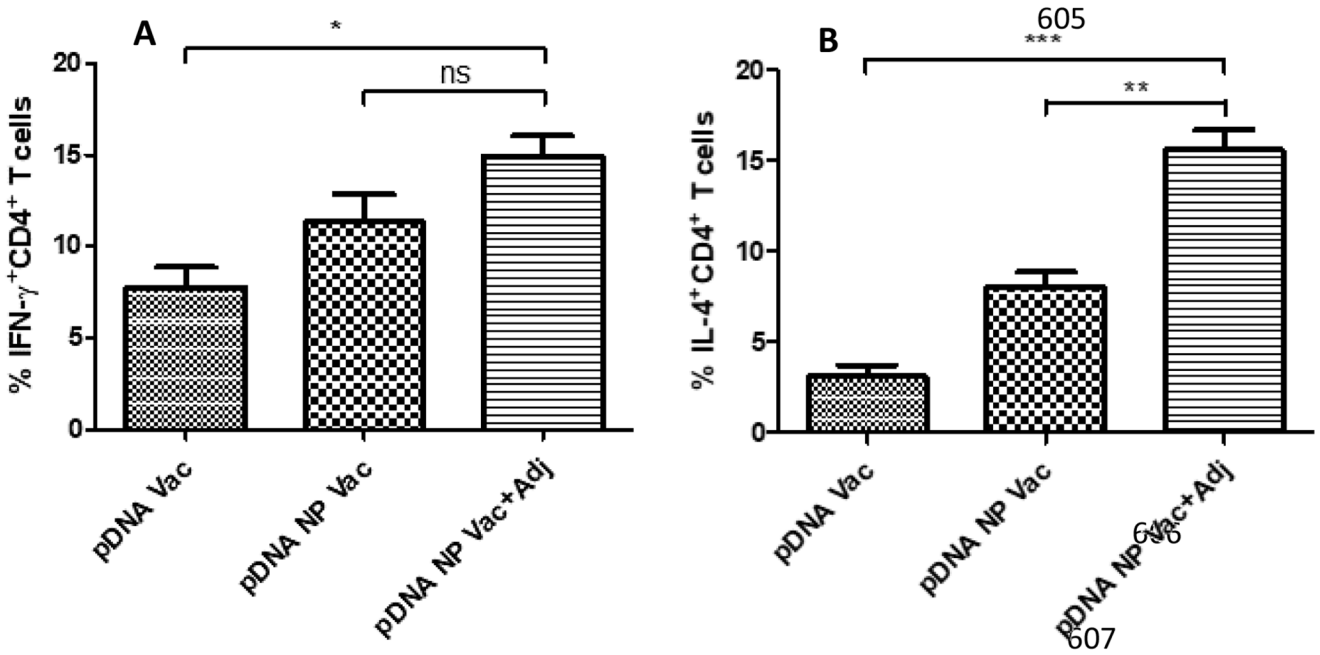

Figure 10 –.

Induction of IFN-ϒ and IL-4 cytokine expressions by $CD4^+$ T cells. Increased expression of IFN-ϒ cytokine results in Th1 mediated cytotoxic immune response and IL-4 cytokine expression dictates Th2 mediated humoral immune response. The cytokine expression was determined by labelling the mice splenocytes with IL-4 and IFN-ϒ antibodies and analyzed via flow cytometry. Results were analyzed using one-way ANOVA followed by post hoc Tukey's multiple comparison test (*$p<0.05$ significant, **$p<0.01$ very significant, ***$p<0.001$ extremely significant). Data are expressed as mean ± SEM, n=3.